JOURNAL OF CATALYSIS 148, 91–99 (1994)

Properties of Tschernichite, the Aluminum-Rich Mineral Analog of Zeolite Beta

R. Szostak,[1,2] K. P. Lillerud, and M. Stöcker*

*Department of Chemistry, University of Oslo, P.O. Box 1025, Blindern, N-0315 Oslo, Norway; and *SINTEF-SI, Oslo, Norway*

Received August 26, 1993; revised January 19, 1994

The physical and hydrothermal properties of natural zeolite tschernichite, an aluminium-rich analogue of the catalytically important zeolite beta, have been examined. Unlike the compositionally similar zeolite Y, the ammonium form of tschernichite is thermally stable to temperatures as high as 900°C. Like synthetic beta, this zeolite dealuminates readily with steam treatment (1 hr, 100% steam, 550°C). Crystallinity is decreased by 30% after steaming but tschernichite maintains its large pore adsorption properties. Dealumination produces a framework that is more silica rich than similarly dealuminated zeolite Y and the dealuminated form exhibits properties similar to as-synthesised beta. The ^{29}Si NMR, framework infrared spectra, and isopropylamine decomposition studies of dealuminated tschernichte further confirm the similarity between this mineral and synthetic beta. © 1994 Academic Press, Inc.

INTRODUCTION

The highly successful commercial zeolite Y is one of the few three-dimensional large pore zeolites known (1). Zeolite beta, synthesised in the 1960's, has only recently been identified as another member of the three-dimensional large pore class of zeolites (2–4). Zeolite beta has been proposed to have good activity and selectivity for numerous catalytic reactions (5–11). Difficulties arise in the direct comparison of the acid properties of beta and zeolite Y due to the large disparity in the SiO_2/Al_2O_3 ratios of the synthesised materials. Zeolite Y crystallises with a SiO_2/Al_2O_3 ratio around six, while beta zeolite crystallises with a minimum ratio around 20. Thus comparisons must be made between dealuminated Y and synthetic beta. This may not be ideal.

Recently, the natural structural analogue of zeolite beta has been identified (12–14). This material, called tschernichite, contains a low SiO_2/Al_2O_3 ratio more closely matching that of synthetic zeolite Y. Its similarity with respect to the composition of zeolite Y makes it a more appropriate material for direct comparison. Understanding the physical properties of this material may provide the missing link needed to compare the properties of a high silica Y-type zeolite (USY) prepared via secondary synthesis methods and high silica beta prepared by direct synthesis. The physiochemical properties of this mineral have not been previously explored and are described in this paper.

EXPERIMENTAL PROCEDURE

Samples of rocks containing tschernichite from Goble, Oregon, USA were received from R. Tschernich of Snohomish, Washington, USA. The tschernichite crystals were found to be loosely attached to the lining of cavities, or vugs, within the rock samples and could be carefully removed with a fine pick. A loose amorphous material (confirmed by isolating a sufficient size sample and subjecting it to powder X-ray diffraction examination) was found between the tschernichite and the rock. It was brushed away so that only pure specimens of tschernichite would be recovered. The individual rock samples weighted between 10 and 20 g with each sample containing between 0.005 and 0.03 g of tschernichite. Next, 1.2 kg of rock was processed resulting in 2.04 g of tschernichite. The zeolite was ground to a fine powder and washed with boiling water. The stir bar used picked up bits of stray magnetic impurities from the rock. The washed sample was then ion exchanged twice with 20 g $NaNO_3$ in 120 g of water. It was then converted to the ammonium form through further ion exchange using 20 g NH_4NO_3 in 120 g of hot water. This procedure was repeated. The final weight of sample after ion exchange and rinsing with 100 ml of distilled water was 1.8 g. The sample is referred to as NH_4Tsch.

Zeolite beta was synthesised as follows: Four hundred grams of tetraethyl ammonium hydroxide (20%, Fluka) was mixed with 4.26 g sodium aluminate (34% Al, 34.3% Na, Kebo). The mixture was stirred until the sodium aluminate dissolved. To this mixture was added 125.8 g of

[1] Present address: Department of Chemistry, Clark Atlanta University, 223 James P. Brawley Dr. SW, Atlanta, GA, 30314.

[2] To whom correspondence should be addressed.

0021-9517/94 $6.00

tetraethyl orthosilicate. This was stirred for 1 hr. The temperature on the hot plate was then increased to near boiling to allow the ethanol to evaporate. This procedure took 4–6 hr. Approximately 15–20 ml of gel was poured into 30-ml capacity Teflon-lined autoclaves and heated to 150°C for 12 days. The resulting solid was filtered, washed with 100 ml of water, dried in air at 150°C, and calcined for 6 hr in dray air at 550°C to remove the residual organic amine. X-ray powder diffraction confirmed the presence of a pure beta phase.

The ammonium forms of beta and tschernichite were steamed under identical conditions using a tube furnace controlled to maintain a temperature of 550°C in which the water vapour was introduced from an attached flask of boiling water. No carrier gas was used to transport the steam. The samples were introduced to the furnace when the steaming conditions (550°C, 100% steam) were attained. Steaming time was 1 hr at these conditions. The steamed samples were subsequently washed with ammonium nitrate solution (10 g NH_4NO_3/100 g H_2O) by stirring at 60–80°C for 1 to 2 hr to remove soluble nonframework aluminium. This also regenerated the ammonium ion exchanged form.

The X-ray powder diffraction data was collected on a Siemens D500 powder diffractometer. It was equipped with a germanium primary monochromator to ensure strictly Kal Cu radiation, an automatic aperture slit and a Bhüler high-temperature sample holder for measurements under controlled atmosphere and temperature. All XRD data were collected on the NH_4 forms of both tschernichite and beta.

The identification of faulted phases in the powder XRD may be even more difficult than the identification of physical mixtures. Newsam *et al.* (2) have described and utilised a computer program (DIFFaX) to simulate diffraction patterns of faulted phases such as zeolite beta. Their work shows that the pattern derived from such faulting is not a linear combination of the patterns of the end members. In Ref. (2), an example of the methodology used in the DIFFaX calcuations for the beta series is presented, going from pure polytype A to pure polytype B assuming a random distribution of the layers. It is apparent that the pattern from an approximately 50 : 50 random stacking of the two phases is nearly identical to the pattern of synthetic beta. This computational approach was used in this work (15).

Prior to adsorption studies, the zeolites, in their ammonium form, were heated in the TGA (Stanton Redcroft 785 TGA/DSC) to 500°C at a rate of 20°C/min to remove water and decompose the ammonium cations, and thus generate the acid form. The hydrocarbon adsorbates used in this study were purchased, purim, from Merck. Flowing nitrogen was saturated with the adsorbate by passing the gas through a column filled with 10 cm^3 of the liquid hydrocarbon at room temperature (ca. 20°C) and flowed over the sample which was maintained at temperatures between 50 and 75°C. Within this range of temperature, pore filling is achieved. Capacity was determined when steady state was reached. A fresh sample of zeolite was used for each hydrocarbon examined. Crystallinity loss upon steam treatment was determined as a percentage calculated from the difference between the adsorption capacity for *n*-hexane before and after steaming relative to the adsorption capacity of the material before steam treatment.

Isopropyl amine (IPA) adsorption/decomposition data was collected in a similar manner. However, adsorption was not allowed to go to saturation but only allowed to adsorb to a weight slightly greater than the weight calculated to be equivalent to one isopropyl amine per one aluminium in the sample based on bulk chemical analysis. The temperature at which the isopropyl amine was adsorbed was 100°C. The temperature of the sample was increased to 200°C and held for 15 to 30 min to remove weakly absorbed amine. No further desorption of the amine was observed until decomposition of the organic occurred when the sample was heated to 350°C. The decomposition was monitored with a mass spectrometer.

Infrared spectra were recorded on a Brucker model 88 FTIR spectrometer covering the regions 4000 to 400 cm^{-1}. Ten wt.% zeolite was used in dry KBr and pressed into a transparent wafer.

The ^{29}Si NMR spectra were recorded on a Bruker CXP-200 pulse Fourier transform NMR spectrometer operating at 39.7 MHz. The spectrometer was fitted with a magic angle spinning probe with a D-poly(methylmethacrylate) rotor spinning at 3.0 kHz. Using a 30° pulse angle (4.1 μs) with 6.5 s repetition time, 8 K data points were recorded over a spectral width of 20 kHz. Three thousand scans were recorded per spectrum and 10-Hz line broadening was applied. Chemical shifts were determined relative to external $Si(CH_3)_4$.

RESULTS AND DISCUSSION

X-Ray Powder Diffraction

Zeolite beta has been previously shown to be composed of a nearly 50 : 50 intergrowth of two polytypes identified as polytype A and polytype B (2–4). X-ray powder diffraction confirms the purity of the tschernichite as no other crystalline phase was detected. The diffraction pattern bears a striking resemblance to the diffraction pattern of zeolite beta as previously reported (13, 14). Data obtained from high-temperature X-ray powder diffraction of NH_4Tsch, which results in a more representative diffraction pattern of the tschernichite lattice without adsorbed water or heavy cations, can be compared with the simu-

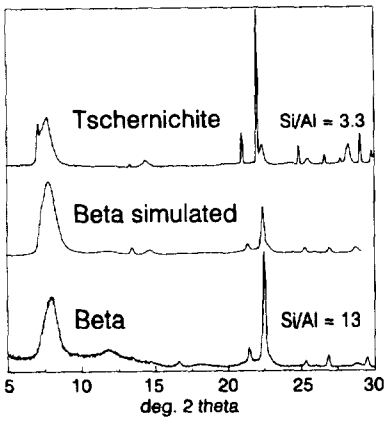

FIG. 1. Comparison of the X-ray powder diffraction pattern recorded at 200°C of NH_4Tsch (top), NH_4beta (bottom) and the simulated diffraction pattern for the intergrowth of beta polytypes A and B (middle) (15).

lated diffraction pattern of beta. Both materials exhibit a mixture of broad and sharp lines in their diffraction pattern, which is indicative of extensive faulting in the crystals. A comparison of the simulated diffraction pattern of beta polytypes A and B and the high-temperature diffraction patterns for NH_4Tsch and NH_4beta are shown in Fig. 1. The position of the reflections in tschernichite shifts to higher *d* spacing relative to those in zeolite beta. This is a result of the differences in the composition. Tschernichite contains a substantial amount of framework aluminium in addition to silica.

The degree of faulting in tschernichite relative to zeolite beta is an important question. Line broadening in general can reflect either a difference in the size of the faulted domains within the crystal or a difference in the size of the crystal itself. A difference in the line width is observed in the diffraction pattern of beta when compared with natural tschernichite. Tschernichite contains sharper reflections than those observed in the XRD of synthetic beta. Zeolite beta generally crystallises in very small agglomerates which are on the order of 1 μm. Thus, in zeolite beta, both line broadening due to the presence of extreme faulting and further broadening due to the small crystallite size occur. Tschernichite, on the other hand, forms large crystals which are approximately an order of magnitude larger than the synthetic counterpart. It would therefore be reasonable to expect some differences in line width due to the physical difference in crystal size. Using the DIFFaX software we confirm that these differences are due to crystal size and that the XRD patterns of beta and tschernichite reflect a similar degree of faulting. Using the parameters for the simulation of highly faulted zeolite beta, an adjustment is made in the line widths for the simulated pattern to account for the larger size of the natural tschernichite crystals. The computed profiles based on different gaussian line widths for the first set of low angle peaks, between 5 and 10° two theta, in the simulated diffraction patterns of beta are shown in Fig. 2 along with profiles of beta (top) and tschernichite (bottom). The intervening figures are that of the simulations using different half widths for the gaussian peaks. The line shape for zeolite beta fits the simulated shape using a peak width of 0.2. Decreasing the half width increasingly sharpens the lower angle peak which is observed only as a shoulder in the very small crystal zeolite beta. Using a gaussian factor of 0.05, which is close to our instrument factor, further sharpens the lower angle peak such that it fits the shape of the larger crystal tschernichite line pattern. No adjustment in the degree of faulting in the crystals was needed.

Tschernichite exhibits excellent thermal stability. Increasing the temperature of the sample in the X-ray powder diffractometer does not adversely influence the diffraction pattern. The diffraction pattern of tschernichite remains viable to temperatures as high as 900°C (*in situ* measurement). No phase change is observed over this

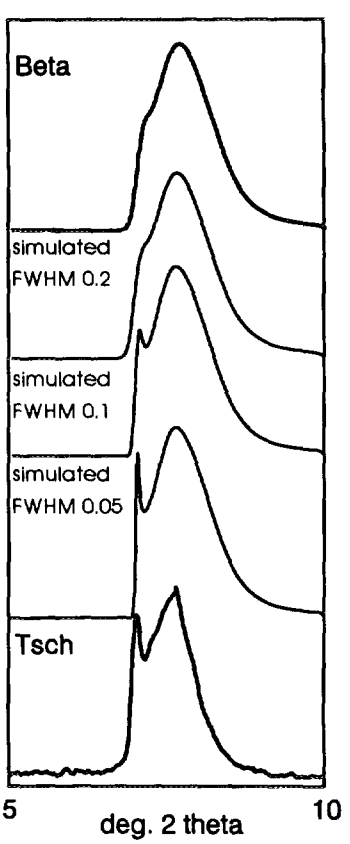

FIG. 2. Simulation of the low angle reflections for beta and tschernichite using different gaussian line widths. The broadening of the low angle peak is due to the small crystal size of synthetic beta (15).

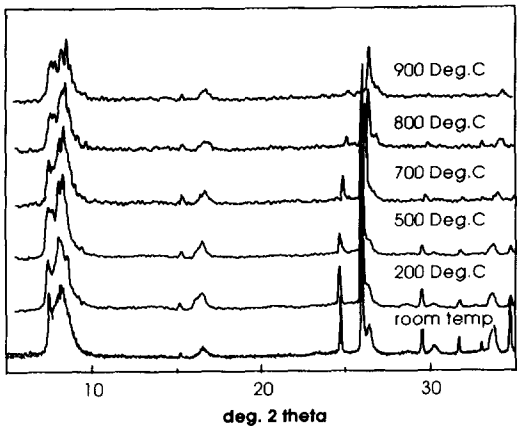

FIG. 3. Series of X-ray powder diffraction patterns for NH_4Tsch taken at temperature intervals between room temperature and 900°C.

range of temperatures. The diffraction patterns for NH_4Tsch at progressively increasing temperature are shown in Fig. 3. Tschernichite exhibits higher thermal stability than its faujasite counterpart. The natural mineral faujasite has been shown by Bennett and Smith to be thermally stable to 475°C; unfortunately, higher temperatures were not reported (16). Zeolite Y (SiO_2/Al_2O_3 = 5) was stable to heating to 760°C, becoming amorphous around 800°C but the NH_4 exchanged form was found to be stable only to 700°C (17–19).

Hydrothermal treatment (1 hr, 100% steam, 550°C) of the ammonium form of tschernichite does not result in any significant changes in the X-ray powder diffraction pattern of the material. Due to a lack of a sufficient number of intense sharp reflections, changes in the crystallinity of the material could not be adequately determined from XRD data. Changes in the adsorption properties were found to be a better indicator of the change in crystallinity. This is discussed in a subsequent section.

Elemental Composition

Analysis of the composition of the tschernichite sample examined in this study indicates a framework that is rich in aluminium. Compositional analysis of all of the samples in this study for Si, Al, Na, and Ca using ICP methods is shown in Table 1. In addition, EDX analysis of a polished cross section of the rock inclusion containing the tschernichite crystals produced a similar silica/alumina composition. No impurities such as iron or magnesium were detected in the sample. It exists naturally as essentially a pure calcium aluminosilicate. It is important to note that the Si/Al ratio of 3.3 of the bulk sample is within the range of compositions found for synthesised zeolite Y. The ammonium ion exchange procedure successfully removed most of the calcium cations present in the natural, as-received mineral, a further indication of the openness of this zeolite's framework toward ion exchange and the absence of any dense insoluble secondary mineral phase.

Hydrothermal treatment and washing with ammonium nitrate causes a slight rise in the bulk silica content of this material. The bulk chemical analysis, however, is not representative of the composition of the zeolite framework. Infrared and NMR results, discussed below, suggest that a strong dealumination of the framework occurs upon hydrothermal treatment. Such disagreement between the bulk composition and the framework composition is commonly observed in other zeolites, most notably dealuminated zeolite Y (20). ^{29}Si NMR and framework infrared spectroscopy are two complementary techniques that provide valuable information on the Si/Al composition of the framework in zeolites.

^{29}Si NMR

^{29}Si NMR has been proven to be an excellent technique to characterise the framework composition of faujasite and dealuminated faujasites (21, 22). Although NMR techniques have been applied to the characterisation of zeolite beta, until now, its quantitative use was limited by the complexity of the beta framework (2–4, 23). Zeolite beta differs significantly from faujasite contains one T site, while beta contains nine. Simulating the ^{29}Si NMR spectrum of faujasite with different Si/Al ratios is simplified as the resonances observed correspond to Si(xAl), where x is between 0 and 4. Although others have reported the ^{29}Si NMR spectra of zeolite beta (23), simulations of those spectra based on the proper number of inequivalent T atom sites, to more accurately predict framework aluminium content, have not been attempted. In the aluminium-rich tschernichite, it is critical to fit the data to the more complex pattern, in order to obtain reasonably accurate account of all framework aluminium.

Fyfe *et al.* (24) have reported the line positions for the nine band ^{29}Si NMR pattern for an all silica framework beta. In this aluminium-rich tschernichite sample with Si/Al = 3, each of the nine unique silicon would potentially

TABLE 1

Bulk Molar Elemental Compositions of Tschernichite and Beta Samples Examined in this Study

	Si	Al	Na	Ca
NH_4Tsch	3.3(3.3)	1	0.02	0.04
Steamed NH_4Tsch	3.5(10)	1	0.07	0.03
NH_4Beta	12.4	1	0.008	—
Steamed NH_4Beta	17.7	1	0.002	—

Note. The silica composition obtained from ^{29}Si NMR is in parentheses.

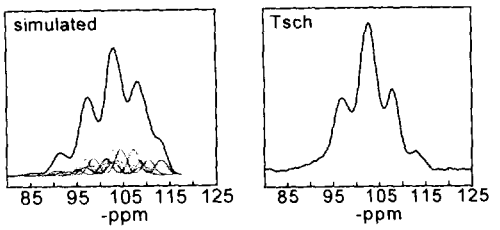

FIG. 4. Comparison of the ^{29}Si NMR spectra of NH_4Tsch and the calculated spectrum accounting for overlaps in the theoretical 45 line pattern.

have, as next nearest neighbours, 0 to 4 Al (Si(xAl); x = 0 – 4). This ultimately gives rise to a 45 peak spectrum. In beta the probability of having Si(xAl) where $x \geq 2$ is diminishingly small and therefore not all of the peaks are observed. Tschernichite would be expected to have significant amounts of Si(xAl) for $x > 2$ and observation of all Si(xAl).

In order to simulate the ^{29}Si NMR of tschernichite, the chemical shifts for the 9 Si(0Al) and their half widths, which were reported by Fyfe *et al.* (24), were used. The intensity ratio used for these lines was based on the structural information presented by Newsam *et al.* for zeolite beta (2) although the intensities reported by Fyfe and coworkers, which were determined prior to the structure determination, were in close agreement with the intensities calculated for the known beta structure.

The addition of aluminium to the framework of beta is expected to broaden and shift the ^{29}Si NMR lines. The average standard value for the line shift associated with Si(xAl), commonly used for faujasite and other zeolites (−5.8 ppm), was used in this simulation (21, 22). Spectra were then calculated by multiplying all line widths by a numerical factor to obtain the best fit to the data. The ^{29}Si NMR spectrum of NH_4Tsch fitted in this way is shown in Fig. 4. Five distinct lines are calculated and only four resolved in the actual spectrum; the fifth line is not resolved. The positions are listed in Table 2 and are compared with the chemical shifts reported by others for zeolite beta. The aluminium content of the framework calculated for tschernichite is 3.3 and matches the bulk Si/Al ratio, indicating that all of the aluminium occupies the tetrahedral lattice sites.

Hydrothermal treatment of both tschernichite and beta results in significant changes in aluminium content of the crystal lattice as seen in the change in the ^{29}Si NMR pattern of tschernichite after treatment. Both tschernichite and beta samples are strongly dealuminated under the conditions used in this study. As aluminium is removed from the framework sites, the ^{29}Si NMR pattern changes to reflect the decrease in the number of Si–O–Al linkages. Although there is only a small change in the bulk SiO_2/Al_2O_3 ratio, the ^{29}Si NMR of hydrothermally with a framework Si/Al ratio around 10. This is now in the range of framework compositions for synthetic beta. In the steamed tschernichite, three signals at −112, −105, and −98 ppm are observed. Only one intense signal at −144 ppm and one very small signal at around −106 ppm are present in steamed beta. These spectra are shown in Fig. 5. Hydrothermal treatment of zeolite Y also results in dealumination and a change in the intensity ratios of the bands in the ^{29}Si NMR (22). Based on a comparison of the framework aluminium content after steaming, tschernichite appears to be more easily dealuminated than zeolite Y. A higher framework silica content (Si/Al) is achieved for tschernichite after one steam treatment, while two treatments are needed for zeolite Y to achieve the same framework aluminium content.

The ^{27}Al NMR spectra of NH_4Tsch, steamed NH_4Tsch, and NH_4beta exhibit only one peak characteristic of aluminium in a tetrahedral framework environment. No evidence for octahedrally coordinated aluminium was found. Further experimental work is needed to characterise the nonframework aluminium component in these samples.

TABLE 2

A Comparison of ^{29}Si NMR Chemical Shifts of Tschernichite

	Si/A	δ(ppm)							
NH4Tsch[a]	3.3		−97.7	−103.4		−108.3			−113.1	
H-beta[b]	11.7	−97			−105		−111			
H-beta[a]	12.4				−105		−111			
H-beta[c]	All silica						−111.1	−112.1	−113	−115.6
							−111.3		−113.1	−115.9
							−111.5			
							−111.7			

[a] This work.
[b] From Ref. (23).
[c] From Ref. (24).

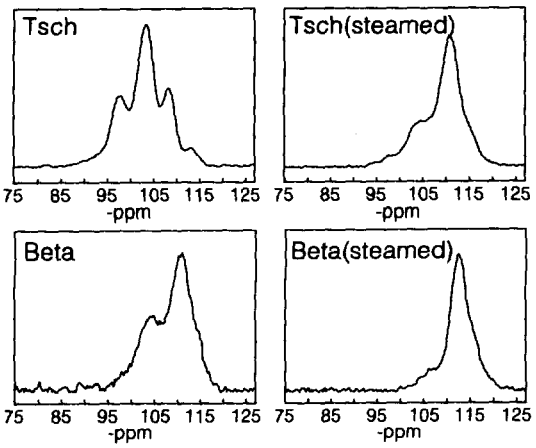

FIG. 5. Comparison of the ^{29}Si NMR spectra of NH_4Tsch (upper left) and steamed NH_4Tech (upper right) with those of NH_4beta (lower left) and steamed NH_4beta (lower right).

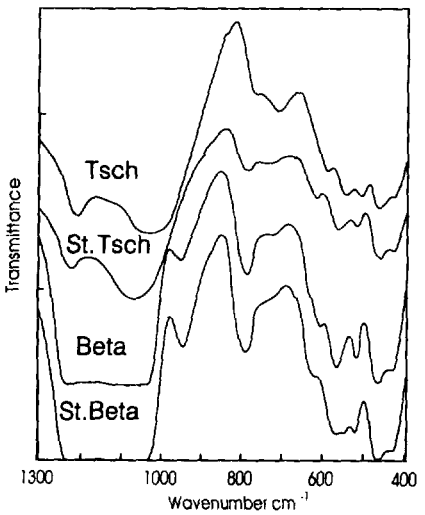

FIG. 6. Framework infrared spectra of NH_4Tsch, steamed NH_4Tsch, NH_4beta, and steamed NH_4beta. The IR spectrum of steamed NH_4Tsch is very similar to that of synthetic beta. The band occurring near 950 cm^{-1} in beta is attributed to silanol groups associated with the lattice. This is not observed in the large crystals of tschernichite.

Framework Infrared Spectra

In order to confirm the framework aluminium contents calculated from the ^{29}Si NMR study, the framework infrared spectra of the beta materials were also examined. Shifts in the infrared framework adsorption bands in the region between 400 and 1300 cm^{-1} to higher frequencies can be related to increasing SiO_2/Al_2O_3 ratio in the crystal structure due either to primary methods of structural silica incorporation (synthesis) or to secondary (dealumination) methods (25). The mid-infrared spectra were recorded for the ammonium forms of tschernichite, steamed tschernichite, beta, and steamed beta. These spectra are compared in Fig. 6. The overall features of the infrared spectra of tschernichite and beta are similar. One extra band is observed in the synthetic sample. That band, appearing at 953 cm^{-1}, is attributed to the presence of silanol groups in the very small crystals of the synthetic phase relative to the natural tschernichite counterpart and may reflect the method of synthesis (25). Newsam *et al.* have suggested that the presence of highly defected silanol sites in beta is in association with faulting of the layers (2). Although similarly faulted, these silanols are absent in the natural sample.

Differences in the peak positions, between tschernichite and beta, are associated with the different amount of framework silica present in the structure. Peak positions for all samples examined are listed in Table 3. The symmetric stretching frequency appearing at 767 cm^{-1} in tschernichite increases in intensity and appears instead at 789 cm^{-1} in the more silica-rich beta. The band at 708 cm^{-1} in tschernichite shifts to higher frequency and is dramatically reduced in intensity, appearing as a shoulder at 730 cm^{-1} in beta. A similar trend is observed after steam treatment of the tschernichite and beta samples. These changes are larger for tschernichite than for beta due to the order of magnitude difference in their SiO_2/Al_2O_3 ratios. The vibration appearing at 767 cm^{-1} in tschernichite increases in intensity and shifts to 786 cm^{-1} upon steaming this material, while the band at 708 cm^{-1} decreases and moves to 742 cm^{-1}. The vibrations at 588, 548, and 506 cm^{-1} all shift to higher frequency. Little change is observed in the bands at 430 and 464 cm^{-1}, as these are insensitive to composition change. When the

TABLE 3

Infrared Spectral Data between 1250 and 400 cm^{-1}

Zeolite	Infrared spectral data (cm^{-1})									
NH_4Tsch	1205	1032		767	708	588	548	507	464	430
Steamed NH_4Tsch	1221	1066		788	742	615	563	519	461	430
NH_4Beta	1223	1080	953	789	730	607	571	523	474	439
Steamed NH_4Beta	1219	1103	945	795	730	611	571	526	470	441

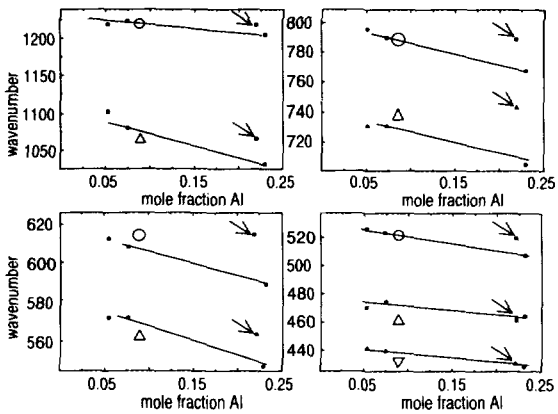

FIG. 7. Correlation of framework vibration shifts with bulk Si/Al ratio (mol fraction Al) for members of the *BEA family. The band positions based on bulk composition of the steamed material are indicated by the solid arrows, while the open markers indicate the same bands replotted using the mol fraction obtained from ^{29}Si NMR.

bulk compositions of the samples under study are plotted as a function of wavenumber (Fig. 7) the steamed tschernichite samples exhibit a larger increase in wavenumber than should be expected if the bulk composition reflected the framework composition. It is apparent from these infrared results that the hydrothermally modified tschernichite contains a more silica-rich lattice than is indicated by the bulk composition of the material. The peak positions for steamed tschernichite can be replotted using the framework aluminium content calculated from the NMR data. The points on the curves in Fig. 7 for steamed tschernichite based on bulk analysis are marked with a solid arrow and those based on NMR framework aluminium are denoted by the open markers. A better fit to the line is observed when the NMR results are used. The infrared results follow those of the ^{29}Si NMR results discussed previously. Steaming of tschernichite results in a material which more closely matching that of the as-synthesised beta. Hydrothermally modified tschernichite would therefore be expected to exhibit properties similar to that of an unsteamed beta sample.

ADSORPTION PROPERTIES

Tschernichite exhibits adsorption properties characteristic of material which contains a large pore structure. These results are shown in Table 4. Nearly equivalent amounts of *n*-hexane and cyclohexane are adsorbed with quantities similar to the adsorption of those molecules in zeolite beta. *n*-Hexane adsorption capacity measurements may be considered to be a more precise method of determining the effect hydrothermal treatment has on the crystal integrity (crystallinity). Based on the adsorption data collected on these samples, dealumination due to steam treatment results in a 29% loss in the tschernichite crystallinity. Unlike tschernichite, negligible loss in crystallinity, based on adsorption capacities, is observed when the higher silica synthetic beta is dealuminated.

TABLE 4

Adsorption Capacities at T = 60–75°C (reported in wt.%)

Zeolite	*n*-Hexane	2,2-DMB[a]	Cyclohexane
HTsch	17.7	—	15
Steamed HTsch	12.5	12.8	—
HBeta	16.2	16.5	17.8
Steamed HBeta	17.3	14.8	—

[a] 2,2-dimethyl-butane.

Water desorption studies reveal a two-step water desorption for the H^+ form of both tschernichite and beta. Both steps occur at similar temperatures in both materials. The weakly bound physically adsorbed water is lost around 180°C, while the more strongly associated water is lost at 360°C. From the water desorption studies it is not possible to discern any difference in the strength of the Brønsted acid sites between these materials.

Isopropyl Amine Adsorption

Temperature-programmed desorption/decomposition has been suggested as an effective measure of the number of Brønsted acid sites in medium and large pore zeolites (26). If the amine is adsorbed on a site capable of catalytically cracking reactions, the amine will be cracked forming propylene and ammonia. It has been previously reported that all sites in zeolite beta associated with framework aluminium are not capable of cracking IPA (27). The necessity for site isolation has been proposed to account for such differences. In aluminium rich zeolites, such as tschernichite, more aluminium next-nearest neighbours may influence the Brønsted acidity as well as the spatial arrangement of the amine adsorbed within this structure. We have observed, from isopropylamine adsorption on HY and HTsch, that half of the framework aluminium is associated with possible Brønsted acid sites, whereas 60% of the aluminium in HY are associated with such sites. These results are summarised in Table 5. It is unclear if the low adsorption amounts for IPA are a result of a decrease in the number of Brønsted sites due to pairing of some of the aluminium ions in the beta framework or to steric factors due to the higher quantities of amine adsorbed on tschernichite relative to beta. Steaming of tschernichite decreases the amount of IPA adsorbed. This decrease of 30%, however, closely follows the loss of crystallinity in the material. As the bulk composition does not reflect the framework aluminium content of the steamed tschernichite, based on the IR and NMR

TABLE 5

Strongly Adsorbed Isopropylamine

Zeolite	wt% ads.[a]	Si/Al	mol IPA/mol Al
HTsch	11.7; 11.1	3.3(3.3[b])	0.5
Steamed HTsch	7.0	3.5(10[b])	1.1[c]
HBeta	7.7; 7.3	12.5	1.0
Steamed HBeta	5.8; 6.2	18	1.1
NH_4Y	15.8; 16.2	2.2	0.6

[a] Calcined at 500°C; calcined at 350°C.
[b] From ^{29}Si NMR.
[c] Correcting for 30% crystallinity loss and Si/Al from NMR ratio of 10.

results discussed above, one can qualitatively conclude that steam treatment with its concomitant decrease in lattice aluminium actually gives rise to an increase in the number of strong Brønsted acid sites which would be associated with the IPA decomposition.

DISCUSSION

Compositionally, only four zeolites containing five member ring building units can be classified as aluminium-rich zeolites. These include bikitaite (SiO_2/Al_2O_3 = 4), epistilbite (SiO_2/Al_2O_3 = 4.6), mazzite (SiO_2/Al_2O_3 = 5.2), and now tschernichite (SiO_2/Al_2O_3 = 6). Only tschernichite represents a three-dimensional large-pore zeolite structure with a synthetic counterpart having commercial possibilities. This aluminium-rich variant of beta exhibits ion exchange and adsorption properties expected for the large-pore structure of beta. No blockage appears to be present in the natural material which could cause a decrease in selective adsorption properties or retention of the counterions. The natural mineral is more thermally stable than zeolite Y. Unlike zeolite Y, tschernichite appears to be more readily dealuminated with steam. Both the infrared and NMR data for the hydrothermally modified tschernichite indicate that the lattice is more silica rich than the bulk compositional analysis indicates, with SiO_2/Al_2O_3 ratios being more closely related to that of the synthesised beta. IPA desorption studies indicate that the number of Brønsted acid sites increases with loss of framework aluminium, which may be due to the loss of next nearest neighbour aluminium ions in the framework which weaken the acid sites in the parent sample. Further identification of the nature of the aluminium in the framework and the Brønsted acid sites is presently underway. The ability of the beta topology to incorporate large amounts of aluminium and to crystallise in the absence of organic amine cations is a new discovery. The existence of such material offers an intriguing starting point and challenge for the synthetic zeolite chemist to produce the synthetic analog of tschernichite. Such a material would exhibit potentially useful catalytic properties.

ACKNOWLEDGMENTS

The authors thank Ms. Anna Horn for obtaining the infrared spectra and the Royal Norwegian Council for Scientific and Industrial Research for support (RS). The authors appreciate the use of the Norsk Hydro license for the Biosym software programs used in this study.

REFERENCES

1. Meier, W. M., and Olson, D. H., "Atlas of Zeolite Structure Types," 3rd ed. Butterworths–Heinemann, London, 1992.
2. Newsam, J. M., Treacy, M. M. J., Koetsier, W. T., and deGruyter, G. B., *Proc. R. Soc. London, A* **420,** 375 (1988); Treacy, M. M. J., Newsam, J. M., and Deem, M. W., *Proc. R. Soc. London, A* **433,** 499 (1991).
3. Treacy, M. M. J., and Newsam, M. J., *Nature (London)* **332,** 249 (1988).
4. Higgins, J. B., LaPierre, R. B., Schlenker, J. L., Rohrman, A. C., Wood, J. D., Kerr, G. T., and Rohrbaugh, W. J., *Zeolites* **8,** 446 (1988).
5. Wadlinger, R. L., Kerr, G. T., and Rosinski, E. J., U.S. Pat. 3,308,069 (1964).
6. Kennedy, C. R., and Ware, R. A., Eur. Pat. Appl. EP186,447 (1986); Chen, N. Y., Ketkar, A. B., Nace, D. M., Kam, A. Y., Kennedy, C. R., and Ware, R. A., Eur. Pat. Appl. EP186,446 (1986); Jorgensen, D. V., and Kennedy, C. R., U.S. Pat. 4,714,537 (1988).
7. Edwards, G. C., and Peter, A. W., Eur. Pat. Appl. EP243,629 (1987).
8. LaPierre, R. B., Partridge, R. D., Chen, N. Y., and Wong, S. S., U.S. Pat. 4,419,220 (1983); LaPierre, R. B., and Partridge, R. D., Eur. Pat. Appl. EP94,827 (1983); LaPierre, R. B., Partridge, R. D., Chen, N. Y., and Wong, S. S., U.S. Pat. 4,518,485 (1985); LaPierre, R. B., and Partridge, R. D., Eur. Pat. Appl. EP 84,827 (1985); LaPierre, R. B., Partridge, R. D., and Wong, S. S., Eur. Pat. Appl. EP214,717 (1987); Garwood, W. E., Le, Q. N., and Wong, S. S., Eur. Pat. Appl. 225,053 (1987).
9. Oleck, S. M., and Wilson, R. C., U.S. Pat. 4,567,655 (1986); Angevine, P. J., Oleck, S. M., Mitchell, K. M., and Shih, S. S., Eur. Pat. Appl. 180,354 (1986).
10. Martens, J. A., Perez-Pariente, J., and Jacobs, P. A., *Acta Phys. Chem.* **31,** 487 (1985).
11. Young, L. B., Eur. Pat. Appl. EP30,084 (1981).
12. Boggs, R. C., Howard, D. G., and Smith, J. V., *Am. Mineral.* **75,** 1200 (1990).
13. Smith, J. V., Pluth, J. J., Boggs, R. C., and Howard D. G., *J. Chem. Soc., Chem. Commun.*, 363 (1991).
14. Tschernich, R. W., "Zeolites of the World," p. 509. Geoscience Press, Phoenix, 1992.
15. Computational results obtained using software programs from Biosym Technologies of San Diego—dynamics calculations from *Dsicover* and graphical display using *Insight II.*
16. Bennett, J. M., and Smith, J. V., *Mater. Res. Bull.* **3,** 633 (1968).
17. Breck, D. W., and Flanigen, E. M., *in* "Molecular Sieves," p. 47. Society of Chemical Industry, London, 1968.
18. Barrer, R. M., and Denny, A. F., *J. Chem. Soc.*, 4684 (1964).
19. Rabo, J. A., Pickert, P. E., Stamires, D. N., and Boyle, J. E., *Actes Congr. Int. Catal., 2nd, 1960* **2,** 2055 (1961).
20. Szostak, R., *Stud. Surface Sci. Catal.* **58,** 153 (1990).
21. Engelhardt, G., Lohse, U., Lippmaa, E., Tarmak, M., and Mägi, M., *Z. Anorg. Allg. Chem.* **482,** 49 (1981).

22. Engelhardt, G., and Michel, D., "High Resolution Solid-State NMR of Silicates and Zeolites." Wiley, Chichester, 1987.
23. Perez-Pariente, J., Sanz, J., Fornes, V., and Corma, A., *J. Catal.* **124,** 217 (1990).
24. Fyfe, C. A., Strobl, H., Kokotailo, G. T., Pasztor, C. T., Barlow, G. E., and Bradley, S., *Zeolites* **8,** 132 (1988).
25. Flanigen, E. M., Khatami, H., and Szymanski, H. A., "Molecular Sieve Zeolites," p. 201. Adv. Chem. Ser. 101, ACS Washington DC, 1971.
26. Gricus Kofke, T. J., Kokotailo, G. T., Gorte, R. J., and Farneth, W. E., *J. Catal.* **115,** 265 (1989).
27. Juskelis, M. V., Slanga, J. P., Roberie, T. G., and Peters, A. W., *J. Catal.* **138,** 391 (1992).